

# Electrochemotherapy of Spinal Metastases Using Transpedicular Approach—A Numerical Feasibility Study

Technology in Cancer Research & Treatment  
Volume 17: 1-13  
© The Author(s) 2018  
Reprints and permission:  
sagepub.com/journalsPermissions.nav  
DOI: 10.1177/1533034618770253  
journals.sagepub.com/home/tct  


Helena Cindrič, BSc<sup>1</sup>, Bor Kos, PhD<sup>1</sup> , Giuseppe Tedesco, MD<sup>2</sup>, Matteo Cadossi, MD, PhD<sup>2</sup>, Alessandro Gasbarrini, MD<sup>2</sup>, and Damijan Miklavčič, PhD<sup>1</sup>

## Abstract

Vertebral column is the most frequent site for bone metastases. It has been demonstrated in previous studies that bone metastases can be efficiently treated by electrochemotherapy. We developed a novel approach to treat spinal metastases, that is, transpedicular approach that combines electrochemotherapy with already established technologies for insertion of fixation screws in spinal surgery. In the transpedicular approach, needle electrodes are inserted into the vertebral body through pedicles and placed around the tumor. The main goal of our study was to numerically investigate the feasibility of the proposed treatment approach. Three clinical cases were used in this study—1 with a tumor completely contained within the vertebral body and 2 with tumors spread also to the pedicles and spinal canal. Anatomically accurate numerical models were built for all 3 cases, and numerical computations of electric field distribution in tumor and surrounding tissue were performed to determine the treatment outcome. Complete coverage of tumor volume with sufficiently high electric field is a prerequisite for successful electrochemotherapy. Close to 100% tumor coverage was obtained in all 3 cases studied. Two cases exhibited tumor coverage of >99%, while the coverage in the third case was 98.88%. Tumor tissue that remained untreated was positioned on the margin of the tumor volume. We also evaluated hypothetical damage to spinal cord and nerves. Only 1 case, which featured a tumor grown into the spinal canal, exhibited potential risk of neural damage. Our study shows that the proposed transpedicular approach to treat spinal metastases is feasible and safe if the majority of tumor volume is contained within the vertebral body. In cases where the spinal cord and nerves are contained within the margin of the tumor volume, a successful and safe treatment is still possible, but special attention needs to be given to evaluation of potential neural damage.

## Keywords

electrochemotherapy, electroporation, numerical modeling, treatment planning, spinal metastases

## Abbreviations

CT, computed tomography; IRE, irreversible electroporation; MR, magnetic resonance; MSE, mean square error; PET/CT, positron emission tomography/computed tomography; RE, reversible electroporation.

Received: September 20, 2017; Revised: December 19, 2017; Accepted: February 22, 2018.

## Introduction

Bone cancers rarely originate from bone tissue or bone marrow but are rather metastasized from a primary tumor elsewhere in the body. Bone metastases usually develop in the later stages of cancer disease, and due to prolonged cancer survival, the number of patients with painful bone metastases has significantly increased in the modern day.<sup>1</sup>

<sup>1</sup> Laboratory of Biocybernetics, Faculty of Electrical Engineering, University of Ljubljana, Ljubljana, Slovenia

<sup>2</sup> Department of Oncologic and Degenerative Spine Surgery, Rizzoli Orthopedic Institute, Bologna, Italy

### Corresponding Author:

Damijan Miklavčič, PhD, Laboratory of Biocybernetics, Faculty of Electrical Engineering, University of Ljubljana, Tržaška cesta 25, 1000 Ljubljana, Slovenia. Email: damijan.miklavcic@fe.uni-lj.si



Vertebral column is the most frequent site for bone metastases. The incidence of spinal metastases in patients with cancer can reach up to 70% depending on primary tumor type. The highest incidence was observed for primary breast cancer, followed by prostate and lung cancer.<sup>2,3</sup> Bone metastases lead to a considerable decrease in patient's quality of life. They cause severe pain, pathological fractures, decreased mobility, neurological disorders as a consequence of hypercalcemia, and in case of spinal metastases, spinal cord, and nerve compression.<sup>1,3</sup>

It is commonly accepted that bone metastases are an expression of a systemic disease and therefore require multidisciplinary treatment. Several options to treat bone metastases are available: radiotherapy, surgery, cryosurgery (as an alternative to conventional surgery), chemotherapy, thermal (radiofrequency) ablation, and sometimes a combination of different therapies is used to achieve better results. The most common treatment option for bone metastases is radiotherapy. More aggressive approaches, such as surgery, are used in case of impending or pathological fractures, huge lesion, and in case of spinal cord compression.<sup>1,4</sup>

Spinal metastases have different shapes and behavior related to the large varieties of histotypes and spread modality of the primary tumor. The choice of the most appropriate treatment is of crucial importance for the patient who may be severely disabled by the presence of untreated spinal metastases. Moreover, these lesions may not only be the cause of severe deterioration in the quality of life but also direct or indirect cause of death. The major goal of treating spinal metastases is restoring spinal stability, cord decompression, and reducing pain. Treatment of spinal metastases is especially complicated because of the importance of vertebral column in bodily support and movement and because of the involvement of spinal cord and nerves. Controversy exists over the most appropriate treatment and despite the evolution of anesthesiological techniques, surgery remains a treatment with many risks and is not always feasible.<sup>5</sup> Therefore, novel and less aggressive treatments for spinal metastases are required, especially for the treatment of patients not responding to standard therapies (eg, radiosensitive tumors), providing patients' relief from symptoms and improving their quality of life.

Electroporation is a technique that uses short intense electrical pulses to induce temporary pores in the cell membrane thus increasing its permeability. Electroporation can be controlled and achieved without compromising cells' viability. Electroporation has become a widespread technique in medicine, food, and biotechnology for facilitating transmembrane transport of larger or low permeant molecules.<sup>6-10</sup>

Electrochemotherapy combines the use of chemotherapeutic drugs with electroporation of the tumor volume, aiming at increasing drug uptake into tumor cells and thus increasing the cytotoxicity of some drugs, such as bleomycin and cisplatin.<sup>11-13</sup> In order for electrochemotherapy to be successful, the whole tumor volume needs to be covered in sufficiently high electric field (reversible electroporation threshold).<sup>14</sup> Various studies have demonstrated that electrochemotherapy is a safe and

effective treatment and is minimally invasive and nontoxic to nontarget tissue. Electrochemotherapy has already been introduced into standard clinical practice and the increasing number of studies confirms its importance in treating cancer disease.<sup>11</sup>

It has been demonstrated in preclinical and clinical studies that bone metastases can be efficiently treated by electrochemotherapy.<sup>15-18</sup> A clinical study was presented by Bianchi *et al*, in which 29 patients were treated with electrochemotherapy in several skeletal sites.<sup>15</sup> There are few human patients with spinal metastases treated by electrochemotherapy, and to our knowledge, only 1 published case, presented by Gasbarrini *et al*.<sup>18</sup> Both clinical studies reported a significant decrease in pain and no adverse neural symptoms associated with the treatment. Furthermore, several preclinical studies have shown that electroporation causes no loss of bone density or cell organization and does not prevent new bone formation.<sup>16,17</sup> There is also evidence of possible bone and nerve tissue regeneration even after irreversible electroporation of tissue (nonthermal ablation).<sup>19,20</sup>

The study presented by Gasbarrini and colleagues<sup>18</sup> is the first reported clinical case using electrochemotherapy to treat spinal metastases. In this case, a partial hemilaminectomy was necessary in order to insert the electrodes directly into the vertebral body. No electrochemotherapy-related adverse events were observed during the procedure and overall improvement in pain outcome and global function after the treatment was excellent. The patient reported preoperative pain intensity of 10 according to visual analog scale, which dropped down to 2 already in the first month after treatment. Moreover, no spinal instability was reported after electrochemotherapy treatment.

The promising results of the first clinical case drove us to further investigate the possibilities for electrochemotherapy treatment for spinal metastases. In this article, we introduce a novel, minimally invasive approach that combines electrochemotherapy with already established technologies for transpedicular insertion of fixation screws in spinal surgery. In the proposed treatment approach, hereinafter referred to as transpedicular approach, needle electrodes are inserted into the vertebral body through the pedicles and placed around the tumor. The electrodes used in this approach have shorter conductive parts (1 cm rather than 3 cm) and are gradually retracted from the vertebral body, allowing to cover the tumor volume in segments rather than all at once and to manipulate various treatment parameters during procedure.

The goal of this study was to numerically investigate the feasibility of the transpedicular approach to treat spinal metastases. Three representative clinical cases, with different stages of vertebral body, pedicle, and spinal canal involvement, were used in the study. Anatomically accurate numerical models were built for all 3 cases, and numerical computations of electric field distribution in tumor and surrounding tissue were performed to determine the outcome of the proposed treatment. In addition to tumor coverage, we also evaluated the hypothetical risk of damage to the spinal cord and nerves.

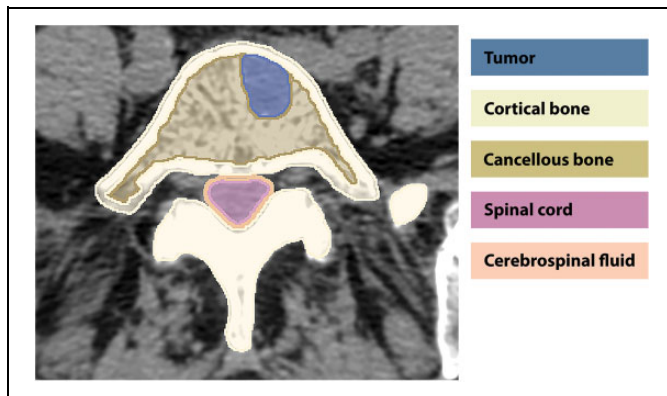


**Figure 1.** An example of tissue segmentation performed on a CT scan of fifth lumbar vertebra with a tumor. All tissues that were not directly included into segmentation were considered as background tissue and were assigned the properties of adipose tissue. CT indicates computed tomography.

## Materials and Methods

We conducted a numerical feasibility study of transpedicular approach to treat spinal metastases. The study was approved by the ethical committee of the Rizzoli Orthopedic Institute (Prot.n.12458/15.05.2009—ES2IOR). All patients gave their written, informed consent to participate in the study. Three representative cases of spinal metastases were used for this study including the case presented by Gasbarrini *et al.*<sup>18</sup> An anatomical model based on medical images was developed for each case. Electrical properties of tissues were determined through an experimental numerical study and applied to the models. Applied voltages were optimized to ensure highest possible tumor coverage. Electric field strength distributions were calculated for each case in order to predict the outcome of the proposed treatment approach.

### Anatomical Models

Geometry for the anatomical models was obtained from computed tomography (CT) and magnetic resonance (MR) scans of patients. 3D Slicer software platform (<https://www.slicer.org/>, Fedorov *et al.*<sup>21</sup>) was used to segment all relevant anatomical structures—tumor tissue, cortical bone, cancellous bone, spinal cord, cerebrospinal fluid, and intervertebral discs. All remaining tissue was considered as background and was assigned the properties of adipose tissue. An example of segmentation of the 5th lumbar vertebra with a tumor is presented in Figure 1.

Segmentation data were imported into Matlab R2016b (MathWorks, Natick, Massachusetts, USA) computing environment where three-dimensional models of the regions of interest were built. The models were based on initial electrical conductivity values and thresholds for reversible and irreversible electroporation of specific tissues found in the literature,<sup>22-28</sup> and numerically determined factors of electrical conductivity increase after electroporation. All tissues were considered homogeneous and isotropic. Osteoporosis effect on dielectric properties of bone tissue is negligible, thus it has

**Table 1.** Electrical Conductivities of Tissues in the Vertebral Column.

Tissue	Initial Electrical Conductivity (S/m)	List of References
Tumor	0.35	22,25,26
Cortical bone	0.02	24,27
Cancellous bone	0.07	23,24
Spinal cord	0.23	27
Cerebrospinal fluid	1.50	23
Intervertebral disc	1.00	28
Background (adipose tissue)	0.02	22

not been accounted for in the models.<sup>29,30</sup> The assigned conductivity values before electroporation, that is initial conductivities, are presented in Table 1, along with the list of the literature from which the data were acquired. In some cases, a combination of different reported values was used due to discrepancies in reported results.

During the delivery of electric pulses, the electrical conductivity of tissues increases due to electroporation. The first approximation of factors of conductivity increase was set to 3.0 for all tissue types<sup>22,25</sup> except for cerebrospinal fluid, conductivity of which was kept unchanged. Factors of conductivity increase were later adjusted through a numerical optimization. The electric field strength threshold for all segmented tissue types was set to 400 V/cm for reversible and 800 V/cm for irreversible electroporation.<sup>25,31-33</sup> The threshold for reversible electroporation of background (adipose) tissue was set to 100 V/cm.<sup>22</sup>

### Numerical Computations

The models were imported into the finite element analysis software Comsol Multiphysics 5.2 (Comsol Inc., Stockholm, Sweden), where all numerical computations were performed. A previously designed numerical framework for treatment planning of deep seated tumors, described in more detail in,<sup>22,34-36</sup> was used for the numerical computations. Live link for Matlab was used to control the method model setup and solving.

Four virtual needle electrodes (1.2 mm diameter and 1 cm conductive length) were inserted into each imported anatomical model as is shown in Figure 2. Two electrodes were inserted through each pedicle and positioned so as to surround the tumor volume. The upper 2 electrodes were parallel to the vertebral body plane while the lower 2 electrodes were positioned at a downward angle with respect to the upper electrodes. Electrode positions were determined based on medical images (CT and MR scans). Electrodes with shorter conductive parts than usual (1 cm rather than 3 cm) are used in this approach allowing us to target the tumor volume more precisely.

The electrodes were connected in pairs resulting in 6 combinations. Electric pulses were applied to each electrode pair. The applied voltage was adjusted based on the distance between centers of electrode tips and was later optimized to ensure highest possible tumor coverage. The minimum applied

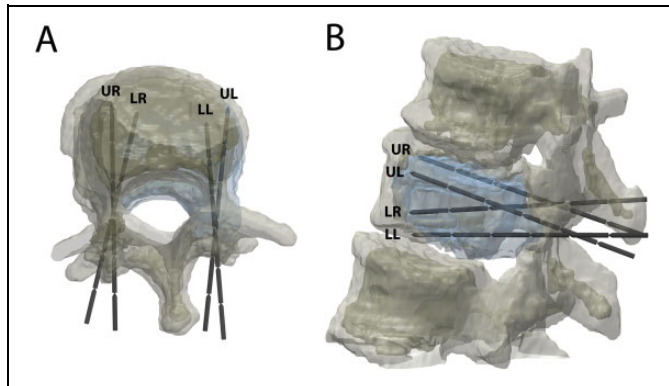


**Figure 2.** An example of electrode placement in the three-dimensional anatomical model of 11th thoracic vertebra in case of transpedicular approach in (A) axial and (B) sagittal view. LL indicates lower left electrode; LR, lower right electrode; UL, upper left electrode; UR, upper right electrode.

voltage was set to 500 V and the maximum to 3000 V since this is the possible range of output voltages provided by currently available devices.<sup>37,38</sup>

Electric field distribution in all tissues and electric currents were calculated after application of pulses to each active electrode pair as previously described.<sup>34,36,39</sup> The model was simplified so that the calculations for each electrode pair were performed independently from other pairs. A train of 8 pulses, delivered to each electrode pair, was modeled as a single pulse; otherwise the conductivity changes between each consecutive pulse in the train would need to be known and modeled.<sup>22</sup> At the beginning of the calculations for each pair, the initial electrical conductivity of all modeled tissues was considered homogenous. The dynamics of conductivity changes and electric fields during each pulse train were then approximated by a sequential model.<sup>39</sup> In each sequence of the model, electric field distribution in tissues was calculated and electrical conductivity values were increased accordingly. Tissue conductivity dependency on electric field distribution was approximated by a sigmoid function. Electrical conductivities defined in each sequence were used to calculate the electric field distribution in the following sequence, thus gradually increasing the total conductivity of tissues throughout the calculation. Our model was based on 6 sequences for each train of pulses. The final electric field distribution at the end of each train of pulses was calculated using the highest values from all previous sequences. Total electric current after the application of pulses was also calculated for each electrode pair.

The transpedicular approach assumes that the tumor volume is covered in segments, with electrodes being retracted a short distance after the application of pulses to all pairs. Upon completion of computations for all 6 active pairs (ie, all possible activations of 4 electrodes), the electrodes were retracted for a distance of 1 cm and computations were performed again. The number of retractions varies from case to case depending on the tumor and vertebra size.

### Optimization of Tissue Conductivity Values

Although there are studies on electrical conductivities of human tissues, the data are scarce and reported results differ between individual studies. In order to develop a numerical model that reflects the conditions in the vertebral column as close as possible, we conducted a numerical study to determine the increase in electrical conductivity due to electroporation for bone and tumor tissue. Two sets of experimental data, published in previous studies,<sup>17,18</sup> were used for this purpose.

**Electrical properties of bone tissue.** Radiological images, acquired during the study of irreversible electroporation of sheep vertebrae,<sup>17</sup> enabled us to delineate a well-defined geometry of the sheep lumbar vertebra with 2 inserted electrodes. Combined with accurate current and voltage measurements for different electroporation protocols used in the procedure, we were able to fine tune the initial values of electrical conductivity and factors of conductivity increase for cortical and cancellous bone.

We designed an algorithm that iteratively changed the factor of conductivity increase for specific bone tissue in order to minimize the absolute error between measured and calculated current. The absolute ( $I_{abs}$ ) and relative ( $I_{rel}$ ) errors were calculated according to:

$$I_{abs} = |I_{meas} - I_{calc}|$$

$$I_{rel} = \left| \frac{I_{meas} - I_{calc}}{I_{meas}} \right|$$

where  $I_{meas}$  is electric current measured during the procedure and  $I_{calc}$  is numerically calculated electric current.

Current measurements of the protocol, that caused little or no electroporation of bone tissue (10 pulses, 100  $\mu$ s, 1000 V),<sup>17</sup> were used to validate the initial conductivity values of bone tissue before electroporation. Current measurements of a second protocol (10 pulses, 100  $\mu$ s, 3000 V), that caused electroporation of bone tissue, were used to determine the factors of conductivity increase.

**Electrical properties of tumor tissue.** In order to determine electrical conductivity values for tumor tissue, we numerically reconstructed the case presented previously.<sup>18</sup> For this purpose, we used the set of intraoperative images, fluoroscopic guidance images, treatment parameters (electrode pairs, distances between electrode tips), and currents and voltages measured during the procedure.

An anatomical model of the 5th lumbar vertebra, which was initially designed for evaluation of electrochemotherapy in case of transpedicular access, was reused for this purpose and adapted accordingly. Two electrodes were inserted through the left pedicle, the other 2 were inserted medially, directly into the vertebral body. Intraoperative images and fluoroscopic control images were used to determine approximate electrode positions. Further optimization of positioning was performed so that the distances, between electrode tips used in computation, matched the distances measured during the procedure as closely as possible (Figure 3). Since it was not registered which

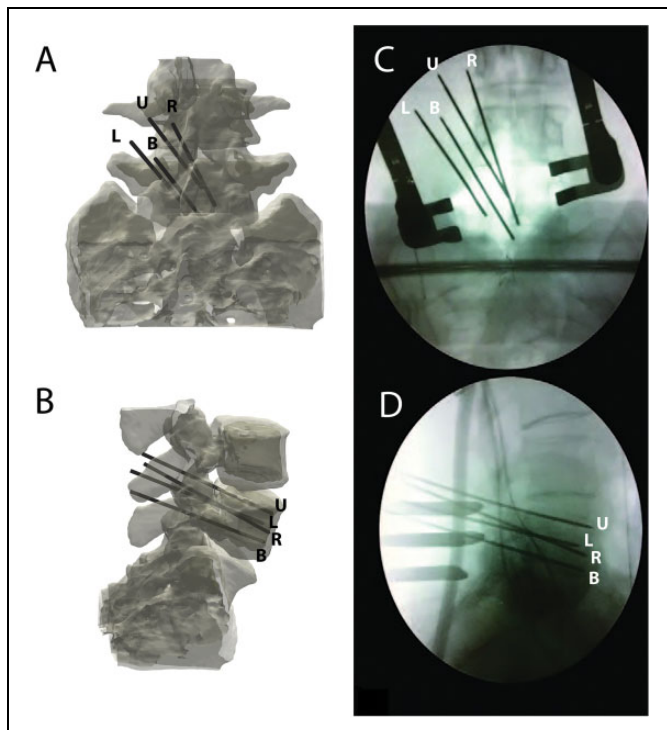


**Figure 3.** (A and B) Numerical reconstruction of the first clinical case of electrochemotherapy of spinal metastases<sup>18</sup>—three-dimensional model of fifth lumbar vertebra with inserted needle electrodes in (A) coronal and (B) sagittal view; (C and D) Fluoroscopic guidance images used in reconstruction of electrode positions. B indicates lower electrode; L, left electrode; R, right electrode; U, upper electrode.

distance corresponded to which electrode pair during operation, we determined the corresponding pairs for computation based on voltages and currents provided. The designed anatomical model with inserted electrodes is presented in Figure 3A and B, next to the fluoroscopic guidance images, which were taken from the study by Gasbarrini *et al*<sup>18</sup> and used for validation of electrode positions (Figure 3C and D).

Electrodes used in this model had a 3-cm-long conductive part and 1.8 mm diameter, mimicking the electrodes used in the actual treatment. The 4 electrodes formed 6 active pairs. The voltage applied to each pair was set to match the voltages used during treatment. Electrical properties of cortical and cancellous bone tissue determined in the sheep experimental study were used in this model.

Electric current and electric field distribution in tissues were calculated for all 6 electrode pairs. Calculated electric currents were then compared to measured electric currents and the mean square error (MSE) between the 2 currents was calculated. Mean square error was calculated according to:

$$\text{MSE} = \frac{1}{n} \sum_{i=1}^n (I_{\text{meas}} - I_{\text{calc}})^2,$$

where  $I_{\text{meas}}$  is electric current measured during the procedure and  $I_{\text{calc}}$  is numerically calculated electric current and  $n$  is the index of the active electrode pair.

The algorithm developed for the sheep experimental study was used to calculate the factor of conductivity increase for tumor tissue by means of minimizing the MSE between the currents.

### Optimization of Applied Voltage Values

The developed numerical models for 3 selected cases with different stages of vertebral body, pedicle, and spinal canal involvement were subjected to further optimization with respect to voltage values delivered to each electrode pair. The first approximation of voltage amplitudes, applied to the electrode pairs, was based on distance between centers of electrode tips. Each value was then optimized using a genetic algorithm.<sup>36,40</sup> The optimization algorithm was set to maximize the volume of the tumor tissue covered with electric field above the reversible threshold and minimize the volume of spinal cord tissue covered with electric field above the irreversible threshold. Applied voltages were varied in 5 steps of 100 V in both directions (lower and higher) from the initially assigned value, resulting in 10 possible values for each electrode pair. The minimum and maximum allowed values were set to 500 V and 3000 V.

First a population of possible candidates for all electrode pairs was generated. Candidates for optimal solution were selected from the population and evolved through 100 generations using operations of the genetic algorithm (crossover, mutations) and the fitness function:

$$F = V_T^{\text{rev}} - V_{SC}^{\text{irr}}$$

where  $F$  is fitness,  $V_T^{\text{rev}}$  is the volume of tumor tissue in  $F = V_T^{\text{rev}} - V_{SC}^{\text{irr}}$  cubic centimeters covered in electric field above the reversible threshold and  $V_{SC}^{\text{irr}}$  is the volume of spinal cord tissue in cubic centimeters covered in electric field above the irreversible threshold.

## Results

In this section, we present numerical results of tissue properties fitting, numerically calculated outcome of the reconstruction of the clinical case, and outcomes of the newly proposed transpedicular approach in 3 different cases of spinal metastases.

### Electrical Properties of Tissues

Electrical properties of tissues, which were defined through the literature survey and numerical optimization, are presented in Table 2. So defined parameters minimized the errors between numerically calculated and actual measured currents for both reconstructed cases—sheep vertebra and Gasbarrini *et al* case. In case of sheep vertebra, the absolute error between calculated and measured current was 0.07 A for the first delivered protocol and 0.02 A for the second delivered protocol. The maximum relative error was 5.68%. Measured and calculated electric currents for both protocols and the absolute and relative errors are presented in Table 3.

**Table 2.** Electrical Properties of Tissues Used in the Numerical Model.

Tissue	Initial Electrical Conductivity (S/m)	Factor of Conductivity Increase After Electroporation (–)
Tumor	0.30	2.80
Cortical bone	0.02	3.00
Cancellous bone	0.07	2.90
Spinal cord	0.23	3.00
Cerebrospinal fluid	1.50	1.00
Intervertebral disc	1.00	3.00
Background	0.02	300

**Table 3.** Comparison of Measured and Calculated Currents for the Preclinical Case Presented Previously.<sup>17</sup>

Electroporation Protocol	Mean Measured Current (A)	Calculated Current (A)	Absolute Error (A)	Relative Error (–)
10 × 100 μs pulses; 1000 V	1.1859	1.1185	0.0674	0.0568
10 × 100 μs pulses; 3000 V	5.9515	5.9714	0.0199	0.0033

For the clinical case, presented by Gasbarrini *et al*, the MSE for calculated and measured electric currents was 2.61 A. Applied voltages, calculated electric currents, actual measured electric currents, and the absolute and relative errors between currents are presented in Table 4. The maximum relative error between measured and calculated current was 16%.

The reconstructed clinical case was also used to validate the adequacy of the designed numerical framework for planning electroporation-based treatments of spinal metastases. The numerical reconstruction predicted 100% (2.13 cm<sup>3</sup>) coverage of tumor tissue with electric field strength equal or greater than the reversible threshold. The cumulative coverage curves for tumor tissue are presented in Figure 4. Each curve represents a volume fraction of tumor tissue with respect to electric field exposure for a single active electrode pair. It can be observed that complete coverage of the tumor with electric field of at least 400 V/cm, that is, reversible threshold, was achieved already after the third applied pulse sequence. After the delivery of pulse sequences to all 6 pairs of electrodes, 0.12 cm<sup>3</sup> of the total spinal cord volume modeled (7.29 cm<sup>3</sup>) was covered with electric field strength above the reversible threshold and 0.016 cm<sup>3</sup> above irreversible threshold.

### Transpedicular Approach

The outcome of the proposed treatment with transpedicular approach has been calculated for 3 cases of spinal metastases with different stages of vertebral body, pedicle, and spinal canal involvement. The cases featured tumors in fifth lumbar vertebra and in the sixth and 11th thoracic vertebrae, respectively.

**Case 1—fifth lumbar vertebra.** The case, which was presented previously<sup>18</sup> and also reconstructed for optimization purposes, presented a solid tumor completely contained within the body of fifth lumbar vertebra. Total volume of tumor tissue in the model was 2.13 cm<sup>3</sup>. Electrodes were retracted once to cover the whole tumor volume with electric field above reversible threshold of 400 V/cm. Figure 5A shows the cumulative coverage curves for tumor tissue. Each curve represents a volume fraction of tumor tissue with respect to electric field exposure for a single active electrode pair (total 12). It can be observed in Figure 5A that approximately 90% of total tumor volume has been covered in sufficiently high electric field already after the third applied sequence of pulses. The remaining part of tumor tissue, positioned in the posterior area of vertebral body, has been covered with application of pulses to the remaining 9 electrode pairs resulting in 99.68% tumor coverage. None of the spinal cord tissue was exposed to electric field high enough to cause electroporation of tissue. The maximum delivered voltage used in this case was 2700 V and the maximum calculated current was 6.96 A.

For this case, we also calculated the outcome of treatment if electrodes with conductive part length of 3 cm were used since this length is common for treating bones. We used the same geometry and electrode positions but without electrode retraction. This treatment plan was submitted to the same optimization algorithm for voltage values as before. Table 5 shows compared results for both treatment plans. Tumor coverage is the same in both cases. No spinal cord tissue was electroporated in either case although the maximum electric field in spinal cord is higher in the case with 3 cm electrodes. The maximum calculated current in case of 3 cm electrodes is almost twice the value of maximum current in the case with 1 cm electrodes.

**Case 2—11th thoracic vertebra.** The second case featured a tumor in the 11th thoracic vertebra that had already grown out of vertebral body, into surrounding tissue, left pedicle, and posterior lamina. Total volume of tumor tissue in the model was 15.53 cm<sup>3</sup>. Electrodes were retracted twice, each time for a distance of 1 cm, covering the tumor volume in 3 segments (deep, medial, and posterior). Coverage of tumor tissue at the end of all 18 applied pulse sequences was 98.88%. The cumulative coverage curves for tumor tissue are shown in Figure 5B. Tumor tissue that remained untreated was positioned on the margin of the tumor near the pedicle area (Figure 6B). The total volume of spinal cord tissue in the model was 7.31 cm<sup>3</sup>, of which 1.228 cm<sup>3</sup> of tissue was exposed to electric field high above reversible threshold and 0.0002 cm<sup>3</sup> above irreversible threshold. The maximum delivered voltage used in this case was 2900 V and the maximum calculated current was 21.33 A.

**Case 3—sixth thoracic vertebra.** In the third case, the tumor was positioned in the posterior part of sixth thoracic vertebral body and had already grown into the pedicles and the spinal canal, compressing the spinal cord. Total volume of tumor tissue in the model was 15.33 cm<sup>3</sup>. Electrodes were retracted twice, each time for a distance of 1 cm, covering the tumor volume in 3 segments.

**Table 4.** Comparison of Measured and Calculated Electric Currents for the Clinical Case Presented Previously.<sup>18</sup>

Electrode Pair	Applied Voltage (V)	Measured Electric Current (A)	Calculated Electric Current (A)	Absolute Error (A)	Relative Error (–)
U-L	1100	8.84	9.89	1.05	0.12
U-R	1000	11.91	10.05	1.86	0.16
U-B	1500	12.88	14.99	2.12	0.16
R-L	1500	14.11	12.79	1.31	0.09
B-L	1700	15.39	17.44	2.05	0.13
B-R	800	7.10	7.91	0.81	0.11

Abbreviations: B, lower electrode; L, left electrode; R, right electrode; U, upper electrode.

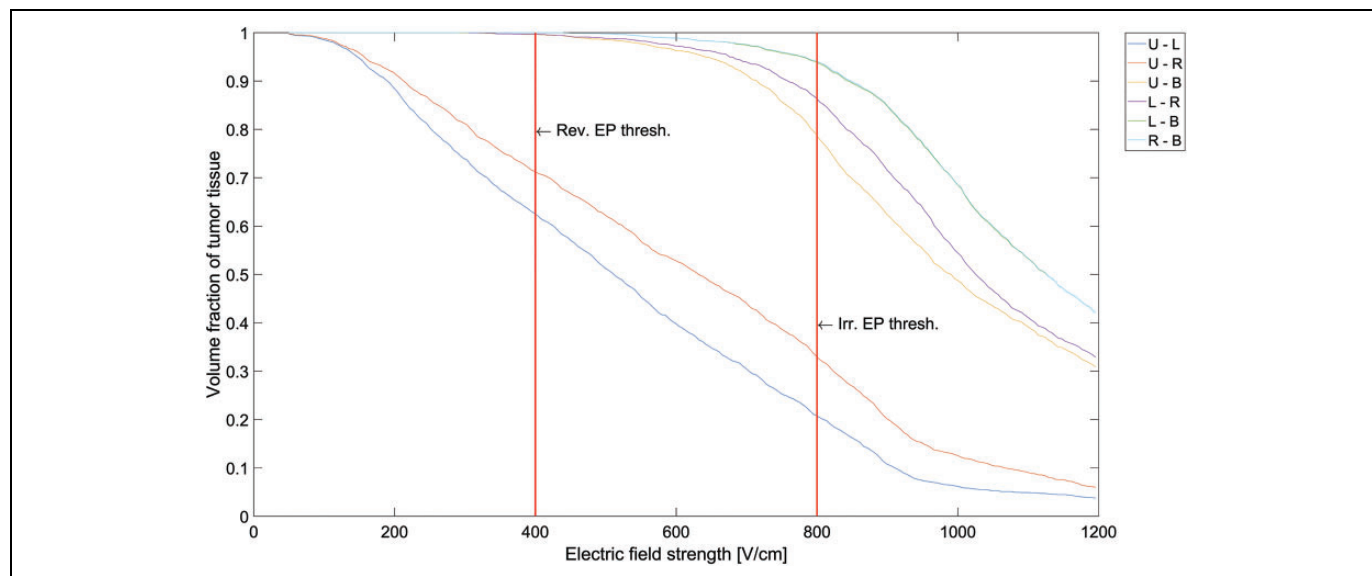


**Figure 4.** Cumulative coverage curves for tumor tissue for the numerically reconstructed clinical case<sup>18</sup> (5th lumbar vertebra). Each curve represents a volume fraction of tumor tissue with respect to electric field strength for a single active electrode pair. B indicates lower electrode; L, left electrode; R, right electrode; U, upper electrode.

The total coverage of tumor tissue was 99.42%. The cumulative coverage curves for tumor tissue are shown in Figure 5C. The total volume of spinal cord tissue in the model was 7.48 cm<sup>3</sup>, of which 1.191 cm<sup>3</sup> of tissue was covered with electric field above the reversible threshold and 0.0124 cm<sup>3</sup> above irreversible threshold. The maximum delivered voltage used in this case was 3000 V and the maximum calculated current was 24.32 A.

Table 6 summarizes the outcomes (total tumor coverage) and other significant parameters for all 3 cases studied, using transpedicular approach. An example of numerically calculated electric field distribution in tumor and bone tissue for all 3 cases is shown in Figure 6. Blue areas represent electroporated tumor tissue while the orange areas represent electroporated bone tissue.

## Discussion

In our study, we investigated feasibility of a novel approach for electrochemotherapy of spinal metastases with the insertion of electrodes through the pedicles, that is, transpedicular approach. For this purpose, we reworked the numerical framework, which was previously designed for planning of

electroporation-based treatments of deep seated tumors, so that it can now also be used for planning of electrochemotherapy of spinal metastases.<sup>22,34</sup> We also investigated the spinal canal involvement and possible risk of neural damage.

Three representative cases have been used in this feasibility study, each showing a different stage of vertebral body, pedicle, and spinal canal involvement. In order for electrochemotherapy to be successful, an adequate concentration of a chemotherapeutic drug and sufficiently high electric field needs to be present in the whole tumor volume.<sup>35</sup> The focus of our study was to investigate the electric field distribution in tumor tissue in case of transpedicular electrode insertion. For this purpose, an individual treatment plan was prepared for each of the 3 cases.

Close to 100% tumor coverage with electric field above reversible threshold value was obtained in all 3 cases. Two cases, fifth lumbar vertebra and sixth thoracic vertebra, exhibited tumor coverage of >99%, while the coverage in 11th thoracic vertebra was 98.88%. In both cases in the thoracic vertebra, the percentage of irreversibly electroporated tumor tissue was quite high, 45% and 63% for the 11th and sixth thoracic vertebra, respectively. It has been revealed in a recent study, however, that threshold value for

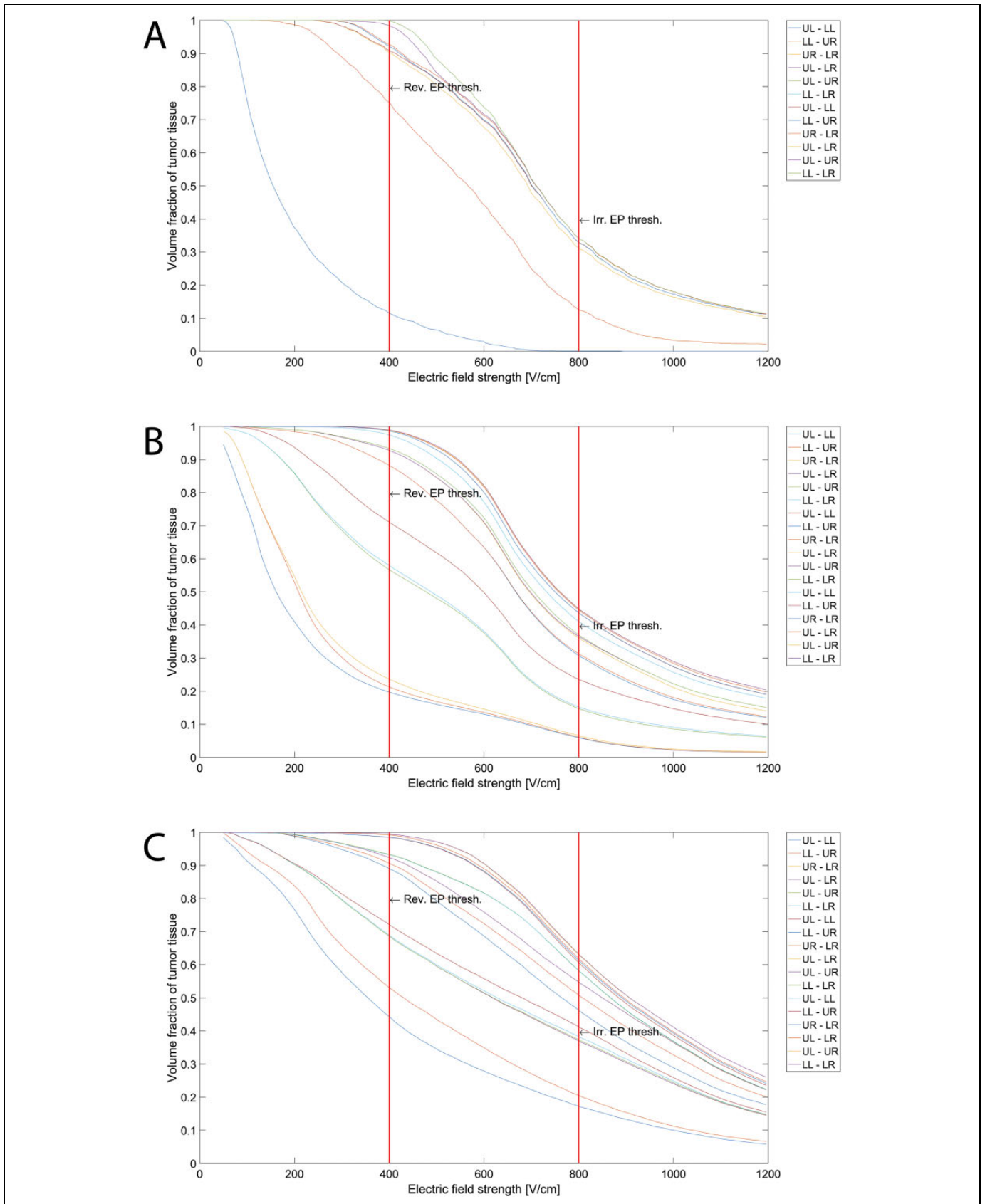


**Figure 5.** Cumulative coverage curves for tumor tissue for 3 studied cases; (A) fifth lumbar vertebra, (B) 11th thoracic vertebra, and (C) sixth thoracic vertebra. Each curve represents a volume fraction of tumor tissue with respect to electric field strength for a single active electrode pair. B indicates lower electrode; L, left electrode; R, right electrode; U, upper electrode.

**Table 5.** Comparison of Treatment for Electrodes With Different Conductive Part Length.

Parameter Description	Electrode Conductive Part Length: 3 cm	Electrode Conductive Part Length: 1 cm
Tumor coverage (%)	99.68	99.68
Maximum delivered voltage (V)	2600	2700
Maximum calculated current (A)	13.44	6.97
Volume of spinal cord tissue above reversible threshold (cm <sup>3</sup> )	0	0
Maximum electric field in spinal cord tissue (V/cm)	230	140

irreversible electroporation of tumor tissue is in fact much higher than threshold values reported in the literature and used in our numerical model (800 V/cm)<sup>41</sup>; therefore, it is likely that the actual percentage of irreversibly electroporated tissue would be lower than that predicted by the model. Preclinical studies have demonstrated that in contrast to other ablative techniques, irreversible electroporation does not affect bone structure in the long term.<sup>16,17,19</sup> It only affects the cell membrane, while the tissue scaffold remains intact, thus preserving the mechanical competence of treated bone. Furthermore, irreversible electroporation does not affect or prevent osteogenic activity. On the contrary, there is emerging evidence that apoptotic cell death caused by electroporation even promotes bone growth and renewal.<sup>20</sup> Nevertheless, further limitations, such as percentage of irreversibly electroporated tumor and bone tissue, could be introduced into the constructed optimization algorithm to prevent unnecessarily high exposure of tissue to electric fields above irreversible threshold. This might result in lower tumor coverage in some cases, but it has been demonstrated in a study on ablation of brain tumors with irreversible electroporation that a complete response is possible even if a fraction of tumor tissue remains untreated.<sup>42</sup> Furthermore, it is also reported in the same study that electric field thresholds that produced good treatment outcomes were lower than the values commonly reported in the literature.

We would also like to point out that although an optimization algorithm was used for applied voltages, electrode positions were determined manually and were not subjected to optimization algorithm. Therefore, a similar algorithm, as was used for optimization of applied voltages, could also be used to optimize electrode positions and would perhaps result in even better tumor coverage. Furthermore, it can be observed in Figure 5 showing cumulative coverage curves for all 3 cases that some electrode pairs do not significantly contribute to total tumor coverage when compared to preceding electrode pairs. An optimization algorithm could identify and exclude such electrode pairs; therefore, it would not only optimize electrode positions to ensure highest tumor coverage but would also minimize exposure of tissues to high electric fields.

An important feature of the transpedicular approach are electrodes with shorter conductive parts. The length of the conductive part of electrodes used in this study was 1 cm

instead of 3 cm, which is currently used for electroporation of bones.<sup>15</sup> Our study on the fifth lumbar vertebra demonstrates that lower maximum currents are delivered when electrodes with shorter conductive parts are used. Furthermore, lower electric field was observed in the spinal canal, which is due to more precise targeting of tumor volume. Also, the overall percentage of electroporated surrounding tissue was lower in case of electrodes with shorter conductive parts.

In constructing numerical models, some limitations need to be acknowledged. The numerical models are based on electrical conductivity values for tissues and factors of conductivity increase due to electroporation. Although there are reports on electrical conductivities of human tissue in the low frequency range needed for electroporation, the data are scarce and the reported results differ considerably between individual studies.<sup>23,24,27,28</sup> The impact of electroporation on conductivity increase is even harder to come by. We thus used 2 sets of experimental data acquired during preclinical and clinical studies of electroporation in vertebra to fine-tune factors of electrical conductivity increase for bone and tumor tissue. Results of the fitting show good agreement between measured and calculated electric currents in tissue, however, further validation is needed. Namely, the data size on which this fitting was performed was small and not acquired specifically for this purpose. More accurate measurements with the exact purpose of investigating the behavior of tissue conductivity subjected to electroporation are thus needed.

The next major uncertainty of the designed model are electroporation thresholds for the treated tumor and surrounding tissues. There are extensive studies on electroporation thresholds for specific tissues, such as liver, muscle, and brain, and on tumors present in these tissues,<sup>25,26,32,43,44</sup> but only a few preclinical studies on the effect of electroporation on bone and nerve tissue.<sup>17,19,27,45,46</sup> Thresholds for bone, bone tumors, and spinal cord have not yet been determined. Reported results on thresholds for electroporation of tumor tissue vary, depending on tumor histology and pulse parameters.<sup>22,25,31,32,43,47</sup> Since there are no reported results on bone tumors, the highest reported threshold for reversible electroporation of tumor tissue was used in this model to prevent overly optimistic prediction of electroporated area. For spinal cord tissue, however, the lowest threshold for irreversible electroporation was used in order to alert of potential risk of neural damage.

Further limitations of the model are mostly related to tissue structure and segmentation complexity. All tissue was considered homogenous and isotropic, although it is known that the actual situation is much more complex—for example, bone tissue, especially cortical bone, is distinctively anisotropic and so is its electrical conductivity.<sup>23</sup> Furthermore, only the most relevant tissues were segmented for the anatomical model. However, previous studies that used a similar modeling approach showed good agreement between calculated and measured data.<sup>25,35</sup>

Upon completion of the model and numerical method setup, the outcome of the reconstructed clinical case presented previously<sup>18</sup> was calculated. Numerical computations

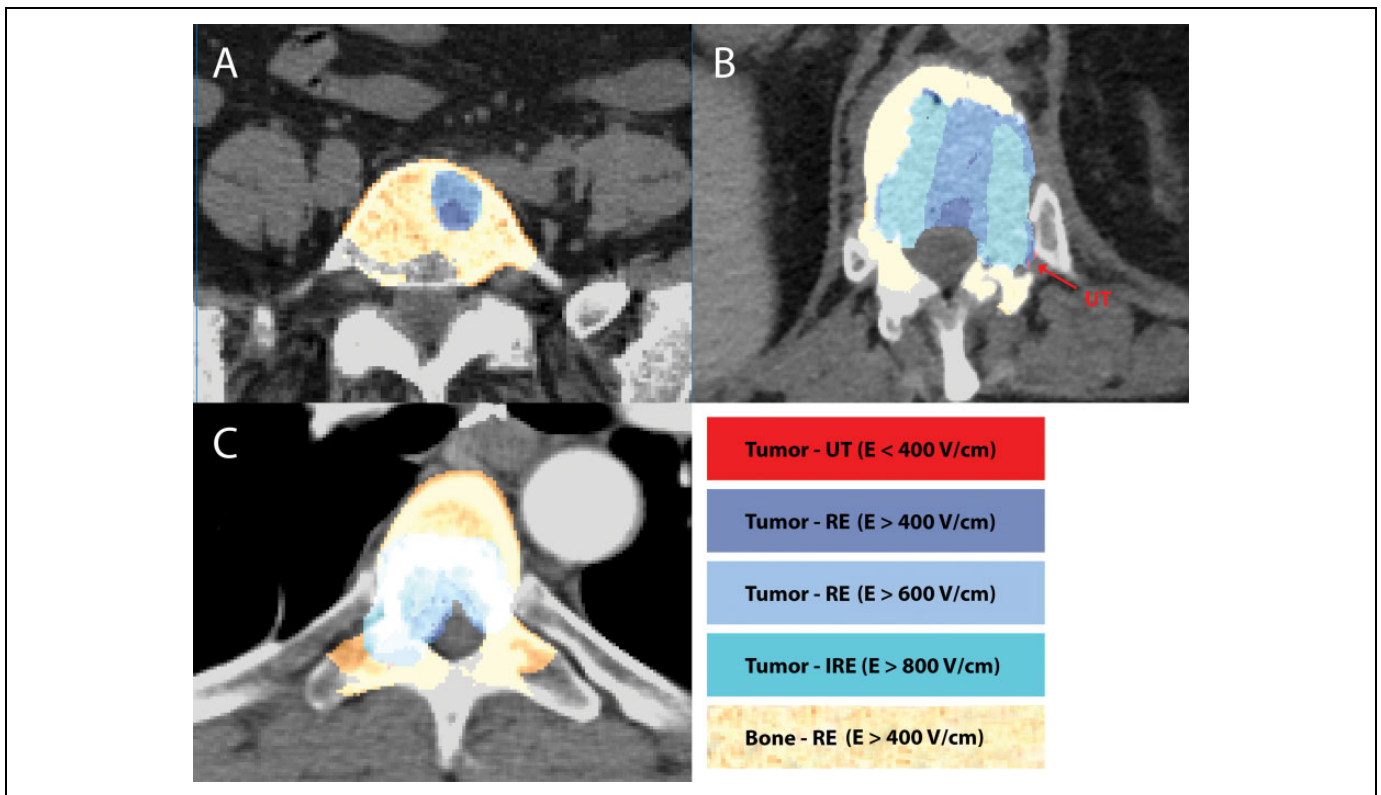


**Figure 6.** Visualization of numerically calculated electric field distribution overlaid onto the corresponding CT images of (A) fifth lumbar vertebra, (B) 11th thoracic vertebra, and (C) sixth thoracic vertebra. The colored areas represent tumor and bone tissue covered in electric field above the reversible electroporation threshold. The arrow indicates some of the untreated tumor tissue in the 11th thoracic vertebra. CT indicates computed tomography; IRE, irreversible electroporation; REP, reversible electroporation; UT, untreated tissue.

**Table 6.** Calculated Treatment Outcomes and Other Significant Parameters.

Patient Case	Total Tumor Coverage (%)	Tumor Coverage Above Irreversible Threshold (%)	Volume of Spinal Cord Tissue Above Reversible Threshold (cm <sup>3</sup> )	Volume of Spinal Cord Tissue Above Irreversible Threshold (cm <sup>3</sup> )	Maximum Electric Field in Spinal Cord Tissue (V/cm)
Case 1: fifth lumbar vertebra <sup>a</sup>	99.68	34.01	0	0	140
Case 2: 11th thoracic vertebra	98.88	44.93	1.228	0.0002	821
Case 3: sixth thoracic vertebra	99.42	63.26	1.191	0.0124	953

<sup>a</sup>The case presented by Gasbarrini *et al.*<sup>18</sup>

predicted 100% tumor electroporation already after the third applied pulse sequence. On the first glance, this result might contradict the actual outcome of the treatment, where a positive positron emission tomography/computed tomography (PET/CT) scan was found at 6-month follow-up which indicated a possible recurrence. However, it has been demonstrated in previous studies that electroporation does not prevent new bone synthesis.<sup>16,19</sup> Moreover, osteogenesis was observed also after irreversible electroporation of the bone.<sup>19</sup> It is thus possible since bone regeneration is associated with increased cell metabolism, that in the Gasbarrini *et al* case, new bone formation was shown in the PET/CT scans rather

than cancer recurrence. But since electrochemotherapy treatment of bone metastases is not yet in clinical practice, preventive measures needed to be taken.

When treating spinal metastases, the potential damage to spinal cord and nerves needs to be considered, especially because both structures are commonly located within the margin of the tumor. Our study showed no electroporation of spinal cord tissue when tumor was located in the anterior part of vertebral body. Both cases in the thoracic vertebra, where the tumor was located also in the posterior part of vertebral body and the pedicles, indicated however some electroporation of spinal cord tissue and possibly some irreversible

electroporation. In both cases, approximately 1 cm<sup>3</sup> of spinal cord tissue was covered with electric field above the assumed threshold for reversible electroporation. It has been demonstrated in a study of single-cell electroporation of neurons that electric properties of recovered cells were indistinguishable from nonelectroporated cells.<sup>48</sup> These findings are also in agreement with the preclinical studies<sup>17,27</sup> and the clinical outcome of the Gasbarrini *et al* case<sup>18</sup> where no long-term adverse effects associated with reversible electroporation were reported. The numerical reconstruction of the clinical case predicted that some of the spinal cord tissue was subjected to electric field high enough to cause reversible and even irreversible electroporation, nevertheless no neural symptoms were observed in the patient. Study of the case in the 11th thoracic vertebra showed that less than 1 mm<sup>3</sup> of spinal cord tissue was exposed to electric field above irreversible threshold. Given the conservative threshold values used in our study, it is probably safe to presume that no neural damage occurred in this case. On the other hand, the case in the sixth thoracic vertebra showed that approximately 12 mm<sup>3</sup> of spinal cord tissue was covered with electric field above the assumed irreversible threshold. These findings could indicate possible neural damage. However, the thresholds used in our numerical study were purposefully conservative in order to prevent overly optimistic outcomes since the effect of reversible and irreversible electroporation of spinal cord tissue has not yet been thoroughly investigated. Recent preclinical studies have shown that the actual threshold for irreversible electroporation of spinal cord and nerve tissue is much higher (at least 1000 V/cm) than the threshold used in our study (800 V/cm), and there is also possible evidence of neural regeneration even after irreversible electroporation.<sup>45,46</sup> Also, a recent study of a direct irreversible electroporation ablation of the spinal canal in pigs<sup>49</sup> showed that irreversible electroporation can be performed directly adjacent to the spinal cord with minimal adverse effects, possibly due to the structure of the spinal canal. The epidural fat surrounding the spinal cord namely acts as a protective layer also in electrical sense. Due to the low electrical conductivity of adipose tissue, the major voltage drop and consequently electric field strength occur in epidural space not in the spinal cord.

Based on our study, we can conclude that with a careful selection of patients, the proposed method to treat spinal metastases with the insertion of electrodes through the pedicles is a feasible approach that should be further investigated. If the majority of tumor volume is contained within vertebral body, the method is minimally invasive and poses minimal risk for neural damage. If the tumor has grown outside of the vertebral body and somewhat into the pedicle area, a successful treatment is still possible but more extensive planning is needed with special attention given to possible involvement of spinal cord and nerves. There is evidence, however, that if the tumor has grown too much into the region of the vertebral arch, we might not be able to cover these regions of tumor volume with sufficiently high electric field without risking damage to the spinal cord tissue. When using needle electrodes, electric field strength drops rapidly with distance from the electrode

surface.<sup>14</sup> In case of transpedicular access, the distance between the electrodes usually increases as we approach insertion point; therefore, it is ever harder to produce electric field high enough to electroporate the tumor volume positioned in the area of vertebral arch. Ever higher voltage amplitudes are needed, which are limited by currently available devices. Another limitation of the approach is our ability to completely surround the tumor with electrodes inserted through the pedicles. The pedicles are mechanically the strongest part of a vertebra but are also the narrowest, and since the electrodes must not penetrate the vertebral wall, we are very limited in terms of positions and angles of the electrodes. Another drawback of electrochemotherapy in bone tissue in general is a difficult follow-up of the treated lesion with standard imaging techniques. Considering that the tumor volume will decrease over time, a close monitoring with MR imaging, CT, or PET/CT becomes necessary to evaluate tumor shrinking.

However, due to many advantages, electrochemotherapy with transpedicular approach could prove to be a successful minimally invasive alternative to other already established treatments of spinal metastases. For example, in the case presented by Gasbarrini *et al*, temporal dislodging of the cauda on the right side after a partial hemilaminectomy was necessary in order to achieve correct electrode positions. In case of transpedicular approach, all 4 electrodes could be inserted through the pedicles and not directly into vertebral body; therefore, laminectomy would not be necessary, thus keeping the treatment minimally invasive. Furthermore, in contrast to other treatment modalities, such as radiotherapy and thermal ablation, electroporation does not cause tissue necrosis and does not compromise bone stability. Neural structures, eventually included in the treatment area, are also far less susceptible to damage caused by electroporation than, for example, to thermal damage. Electrochemotherapy could therefore potentially also be used for the treatment of patients not amenable to other treatments or not responding to standard therapies. The use of electrodes with shorter conductive parts enable targeting tumor tissue more precisely, resulting in minimal damage to the surrounding tissue, and reducing maximum delivered electric currents therefore reducing negative side effects of the treatment. Finally, the transpedicular approach combines electrochemotherapy, which has already proved to be successful in treating other malignancies as well as bone metastases, with insertion of electrodes through the pedicles, which is a similar technique to already established orthopedic procedures. Insertion of fixation screws is the most frequent technique in vertebral fixation surgery.<sup>50</sup> The technology developed for automated screw insertion trajectory planning and intraoperative guidance could thus, with some adaptation, also be used for electrode insertion for electrochemotherapy purpose.<sup>50-52</sup>

Further studies on electrical properties of tissues and effects of reversible and irreversible electroporation on vital anatomical structures are needed to fully understand the limitations and risks of electrochemotherapy to metastases in the vertebrae. However, the results of this numerical feasibility study provide the basis and evidence that should encourage further analysis

and experiments, either additional numerical computations on more samples or experimental studies on animal models. We have shown that electrochemotherapy with transpedicular approach could prove to be a safe and minimally invasive treatment of spinal metastases.

### Authors' Note

This study was conducted within the scope of the European Associated Laboratory on the Electroporation in Biology and Medicine (LEA-EBAM).

### Declaration of Conflicting Interests

The author(s) declared the following potential conflicts of interest with respect to the research, authorship, and/or publication of this article. Damijan Miklavčič holds patents on electrochemotherapy that have been licensed to IGEA S.p.a (Carpi, Italy) and is also consultant to various companies with interest in electroporation-based technologies and treatments. Matteo Cadossi is Vice President of IGEA S.p.A. (Carpi, Italy) and holds 10% of the shares of the Company.

### Funding

The author(s) disclosed receipt of the following financial support for the research, authorship, and/or publication of this article: This study was supported by the Slovenian Research Agency (ARRS) [grant numbers P2-0249, Z3-7126].

### ORCID iD

Bor Kos, PhD  <http://orcid.org/0000-0001-6219-7046>

### References

- Biermann JS, Holt GE, Lewis VO, Schwartz HS, Yaszemski MJ. Metastatic bone disease: diagnosis, evaluation, and treatment. *J Bone Joint Surg Am*. 2009;91(6):1518-1530.
- Choi D, Crockard A, Bungler C, et al. Review of metastatic spine tumour classification and indications for surgery: the consensus statement of the Global Spine Tumour Study Group. *Eur Spine J*. 2010;19(2):215-222. doi:10.1007/s00586-009-1252-x.
- Weilbaecher KN, Guise TA, McCauley LK. Cancer to bone: a fatal attraction. *Nat Rev Cancer*. 2011;11(6):411-425. doi:10.1038/nrc3055.
- Ecker RD, Endo T, Wetjen NM, Krauss WE. Diagnosis and treatment of vertebral column metastases. *Mayo Clin Proc*. 2005; 80(9):1177-1186. doi:10.4065/80.9.1177.
- Sundaresan N, Rothman A, Manhart K, Kelliher K. Surgery for solitary metastases of the spine: rationale and results of treatment. *Spine*. 2002;27(16):1802-1806.
- Rems L, Miklavčič D. Tutorial: electroporation of cells in complex materials and tissue. *J Appl Phys*. 2016;119(20):201101. doi:10.1063/1.4949264.
- Yarmush ML, Golberg A, Serša G, Kotnik T, Miklavčič D. Electroporation-based technologies for medicine: principles, applications, and challenges. *Annu Rev Biomed Eng*. 2014;16: 295-320. doi:10.1146/annurev-bioeng-071813-104622.
- Kotnik T, Frey W, Sack M, Haberl Meglič S, Peterka M, Miklavčič D. Electroporation-based applications in biotechnology. *Trends Biotechnol*. 2015;33(8):480-488. doi:10.1016/j.tibtech. 2015.06.002.
- Mahnič-Kalamiza S, Vorobiev E, Miklavčič D. Electroporation in food processing and biorefinery. *J Membr Biol*. 2014;247(12): 1279-1304. doi:10.1007/s00232-014-9737-x.
- Golberg A, Sack M, Teissie J, et al. Energy-efficient biomass processing with pulsed electric fields for bioeconomy and sustainable development. *Biotechnol Biofuels*. 2016;9(1):94.
- Miklavčič D, Mali B, Kos B, Heller R, Serša G. Electrochemotherapy: from the drawing board into medical practice. *Biomed Eng Online*. 2014;13(1):29. doi:10.1186/1475-925X-13-29.
- Sersa G, Cemazar M, Miklavcic D. Antitumor effectiveness of electrochemotherapy with cis-diamminedichloroplatinum(II) in mice. *Cancer Res*. 1995;55(15):3450-3455.
- Orlowski S, Belehradek J, Paoletti C, Mir LM. Transient electropermeabilization of cells in culture: increase of the cytotoxicity of anticancer drugs. *Biochem Pharmacol*. 1988;37(24):4727-4733. doi:10.1016/0006-2952(88)90344-9.
- Miklavčič D, Čorović S, Pucihar G, Pavšelj N. Importance of tumour coverage by sufficiently high local electric field for effective electrochemotherapy. *Eur J Cancer Suppl*. 2006;4(11):45-51. doi:10.1016/j.ejcsup.2006.08.006.
- Bianchi G, Campanacci L, Ronchetti M, Donati D. Electrochemotherapy in the treatment of bone metastases: a phase II trial. *World J Surg*. 2016;40(12):3088-3094. doi:10.1007/s00268-016- 3627-6.
- Fini M, Salamanna F, Parrilli A, et al. Electrochemotherapy is effective in the treatment of rat bone metastases. *Clin Exp Metastasis*. 2013;30(8):1033-1045. doi:10.1007/s10585-013-9601-x.
- Tschon M, Salamanna F, Ronchetti M, et al. Feasibility of electroporation in bone and in the surrounding clinically relevant structures: a preclinical investigation. *Technol Cancer Res Treat*. 2016;15(6):737-748. doi:10.1177/1533034615604454.
- Gasbarrini A, Campos WK, Campanacci L, Boriani S. Electrochemotherapy to metastatic spinal melanoma: a novel treatment of spinal metastasis? *Spine*. 2015;40(24): E1340-1346. doi:10.1097/BRS.0000000000001125.
- Fini M, Tschon M, Ronchetti M, et al. Ablation of bone cells by electroporation. *J Bone Joint Surg Br*. 2010;92(11):1614-1620. doi:10.1302/0301-620X.92B11.24664.
- Song Y, Zheng J, Yan M, et al. The effect of irreversible electroporation on the femur: experimental study in a rabbit model. *Sci Rep*. 2015;5:18187. doi:10.1038/srep18187.
- Fedorov A, Beichel R, Kalpathy-Cramer J, et al. 3D Slicer as an image computing platform for the quantitative imaging network. *Magnetic Resonance Imaging*. 2012;30(9):1323-1341.
- Kos B, Županič A, Kotnik T, Snoj M, Serša G, Miklavčič D. Robustness of treatment planning for electrochemotherapy of deep-seated tumors. *J Membr Biol*. 2010;236(1):147-153. doi:10.1007/s00232-010-9274-1.
- Gabriel C, Peyman A, Grant EH. Electrical conductivity of tissue at frequencies below 1 MHz. *Phys Med Biol*. 2009;54(16):4863. doi:10.1088/0031-9155/54/16/002.
- Gabriel C, Gabriel S, Corthout E. The dielectric properties of biological tissues: I. Literature survey. *Phys Med Biol*. 1996; 41(11):2231-2249.
- Pavšelj N, Bregar Z, Cukjati D, Batiuskaite D, Mir LM, Miklavčič D. The course of tissue permeabilization studied on a

- mathematical model of a subcutaneous tumor in small animals. *IEEE Trans Biomed Eng.* 2005;52(8):1373-1381. doi:10.1109/TBME.2005.851524.
26. Cukjati D, Batiuskaite D, André F, Miklavcic D, Mir LM. Real time electroporation control for accurate and safe in vivo non-viral gene therapy. *Bioelectrochemistry Amst Neth.* 2007; 70(2):501-507. doi:10.1016/j.bioelechem.2006.11.001.
  27. Tam AL, Abdelsalam ME, Gagea M, et al. Irreversible electroporation of the lumbar vertebrae in a porcine model: is there clinical-pathologic evidence of neural toxicity? *Radiology.* 2014;272(3):709-719. doi:10.1148/radiol.14132560.
  28. IT'IS Foundation. Low frequency (conductivity). <https://www.itis.ethz.ch/virtual-population/tissue-properties/database/low-frequency-conductivity/>. Accessed August 19, 2017.
  29. Barger-Lux MJ, Recker RR. Bone microstructure in osteoporosis: transilial biopsy and histomorphometry. *Top Magn Reson Imaging.* 2002;13(5):297-305.
  30. Williams PA, Saha S. The electrical and dielectric properties of human bone tissue and their relationship with density and bone mineral content. *Ann Biomed Eng.* 1996;24(2):222-233.
  31. Šemrov D, Miklavčič D. Calculation of the electrical parameters in electrochemotherapy of solid tumours in mice. *Comput Biol Med.* 1998;28(4):439-448.
  32. Šel D, Maček Lebar A, Miklavčič D. Feasibility of employing model-based optimization of pulse amplitude and electrode distance for effective tumor electroporation. *IEEE Trans Biomed Eng.* 2007;54(5):773-781. doi:10.1109/TBME.2006.889196.
  33. Kranjc M, Markelc B, Bajd F, et al. In situ monitoring of electric field distribution in mouse tumor during electroporation. *Radiology.* 2015;274(1):115-123. doi:10.1148/radiol.14140311.
  34. Marčan M, Pavliha D, Kos B, Forjanič T, Miklavčič D. Web-based tool for visualization of electric field distribution in deep-seated body structures and planning of electroporation-based treatments. *Biomed Eng Online.* 2015;14(suppl 3):S4. doi:10.1186/1475-925X-14-S3-S4.
  35. Miklavčič D, Snoj M, Županič A, et al. Towards treatment planning and treatment of deep-seated solid tumors by electrochemotherapy. *Biomed Eng Online.* 2010;9:10. doi:10.1186/1475-925X-9-10.
  36. Županič A, Kos B, Miklavčič D. Treatment planning of electroporation-based medical interventions: electrochemotherapy, gene electrotransfer and irreversible electroporation. *Phys Med Biol.* 2012;57(17):5425-5440. doi:10.1088/0031-9155/57/17/5425.
  37. Pirc E, Reberšek M, Miklavčič D. Dosimetry in electroporation-based technologies and treatments. In: *Dosimetry in Bioelectromagnetics*. 1st ed. Boca Raton: CRC Press; 2017:233-268.
  38. Bertacchini C, Margotti PM, Bergamini E, Lodi A, Ronchetti M, Cadossi R. Design of an irreversible electroporation system for clinical use. *Technol Cancer Res Treat.* 2007;6(4):313-320. doi:10.1177/153303460700600408.
  39. Šel D, Cukjati D, Batiuskaite D, Slivnik T, Mir LM, Miklavčič D. Sequential finite element model of tissue electroporation. *IEEE Trans Biomed Eng.* 2005;52(5):816-827. doi:10.1109/TBME.2005.845212.
  40. Županič A, Čorović S, Miklavčič D. Optimization of electrode position and electric pulse amplitude in electrochemotherapy. *Radiol Oncol.* 2008;42(2):93-101.
  41. Kranjc M, Kranjc S, Bajd F, Serša G, Serša I, Miklavčič D. Predicting irreversible electroporation-induced tissue damage by means of magnetic resonance electrical impedance tomography. *Sci Rep.* 2017;7(1):10323. doi:10.1038/s41598-017-10846-5.
  42. Garcia PA, Kos B, Rossmeisl JH, Pavliha D, Miklavčič D, Davalos RV. Predictive therapeutic planning for irreversible electroporation treatment of spontaneous malignant glioma. *Med Phys.* 2017;44(9):4968-4980. doi:10.1002/mp.12401.
  43. Kranjc M, Markelc B, Bajd F, et al. In situ monitoring of electric field distribution in mouse tumor during electroporation. *Radiology.* 2015;274(1):115-123. doi:10.1148/radiol.14140311.
  44. Miklavčič D, Šemrov D, Mekid H, Mir LM. A validated model of in vivo electric field distribution in tissues for electrochemotherapy and for DNA electrotransfer for gene therapy. *Biochim Biophys Acta.* 2000;1523(1):73-83.
  45. Schoellnast H, Monette S, Ezell PC, et al. Acute and subacute effects of irreversible electroporation on nerves: experimental study in a pig model. *Radiology.* 2011;260(2):421-427. doi:10.1148/radiol.11103505.
  46. Schoellnast H, Monette S, Ezell PC, et al. The delayed effects of irreversible electroporation ablation on nerves. *Eur Radiol.* 2013; 23(2):375-380. doi:10.1007/s00330-012-2610-3.
  47. Qin Z, Jiang J, Long G, Lindgren B, Bischof JC. Irreversible electroporation: an in vivo study with dorsal skin fold chamber. *Ann Biomed Eng.* 2013;41(3):619-629. doi:10.1007/s10439-012-0686-1.
  48. Nevian T, Helmchen F. Calcium indicator loading of neurons using single-cell electroporation. *Pflugers Arch.* 2007;454(4):675-688. doi:10.1007/s00424-007-0234-2.
  49. Tam AL, Figueira TA, Gagea M, et al. Irreversible electroporation in the epidural space of the porcine spine: effects on adjacent structures. *Radiology.* 2016;281(3):763-771. doi:10.1148/radiol.2016152688.
  50. Knez D, Mohar J, Cirman RJ, Likar B, Pernuš F, Vrtovec T. Determination of the pedicle screw size and trajectory in CT images of thoracic spinal deformities: a comparison between manual and computer-assisted preoperative planning. *Slov Med J.* 2017;85(11-12). <http://vestnik.szd.si/index.php/ZdravVest/article/view/1747>. Accessed July 18, 2017.
  51. Tian N-F, Huang Q-S, Zhou P, et al. Pedicle screw insertion accuracy with different assisted methods: a systematic review and meta-analysis of comparative studies. *Eur Spine J.* 2011;20(6):846-859. doi:10.1007/s00586-010-1577-5.
  52. Koktekir E, Ceylan D, Tatarli N, Karabagli H, Recber F, Akdemir G. Accuracy of fluoroscopically-assisted pedicle screw placement: analysis of 1,218 screws in 198 patients. *Spine J.* 2014; 14(8):1702-1708. doi:10.1016/j.spinee.2014.03.044.